Novel mechanisms and signaling pathways in angiogenesis

Forghany, Z.

CHAPTER 2

Control of endothelial cell tube formation by Notch ligand intracellular domain interactions with activator protein 1 (AP-1)

J.Biol.Chem.(2017)292(52) 21282–21290

Zary Forghany[1]*, Francesca Robertson[1,4]*, Alicia Lundby[2,3], Jesper V. Olsen[2], David A. Baker

1. Leiden University Medical Center (LUMC), Department of Molecular Cell Biology, 2300 RC Leiden, The Netherlands.
2. Novo Nordisk Foundation Center for Protein Research, Faculty of Health and Medical Sciences, University of Copenhagen, Copenhagen, Denmark.
3. Department of Biomedical Sciences, Faculty of Health and Medical Sciences, University of Copenhagen, Copenhagen, Denmark.
4. University of Oxford, Department of Biochemistry, South Parks Rd, Oxford, OX1 3QU.

*Joint first authors

ABSTRACT

Notch signaling is a ubiquitous signal transduction pathway found in most if not all metazoan cell types characterized to date. It is indispensable for cell differentiation as well as tissue growth, tissue remodelling and apoptosis. Although the canonical Notch signaling pathway is well characterized, accumulating evidence points to the existence of multiple, less well-defined, layers of regulation. In this study, we have investigated the function of the intracellular domain (ICD) of the Notch ligand DLL4. We provide evidence that the DLL4 ICD is cleaved and interacts with the JUN proto-oncogene, which forms part of the activator protein 1 (AP-1) transcription factor complex. Mechanistically, the DLL4 ICD inhibits JUN binding to DNA and thereby controls the expression of JUN target genes, including DLL4. Our work demonstrates that JUN strongly stimulates endothelial sprouting and that DLL4 constrains this process. These data raise the possibility that Notch/DLL4 signaling is bi-directional and suggests that the DLL4 ICD could represent a point of cross-talk between Notch and RTK signaling.

INTRODUCTION

The generic Notch signaling network is a central regulator of cell fate (Kopan and Ilagan 2009; Guruharsha et al. 2012). This pathway is absolutely necessary for normal development and tissue homeostasis and corruption of it has been implicated in numerous diseases including the majority of solid tumors where it plays diverse oncogenic and tumor-suppressive roles (Aster et al. 2017; Braune et al. 2016; Ranganathan et al. 2011). In vertebrates, the Notch signaling system is composed of four single-pass cell surface receptors (Notch1-4) and five Type 1 transmembrane ligands: Jagged (JAG)1, JAG2, Delta-Like (DLL)1, DLL3, and DLL4 (Kopan and Ilagan 2009; Bray 2016; Ulla-Maj and Martinez Arias 2007). Operationally, the canonical Notch signaling pathway is relatively well characterized (Guruharsha et al. 2012; Bray 2016; Ulla-Maj and Martinez Arias 2007). It is activated by a trans interaction between a Notch receptor on one cell and a ligand expressed by a neighbouring cell. This triggers a cascade of proteolytic events terminating in the γ-secretase-mediated cleavage of the Notch intracellular domain which translocates to the nucleus whereupon it regulates expression of Notch target genes (Kopan and Ilagan 2009; Kitagawa 2016). By these means, the molecular and cellular asymmetries required for tissue maintenance and development are established across populations of cells. In recent years, studies have identified manifold, unique facets of Notch signaling (Bray 2006). These include cis receptor/ligand interactions (since each are expressed in the same cell (Del Alamo et al. 2011), ligand-independent signaling (Palmer and Deng 2015), endocytosis of Notch and Notch ligands as an essential mediator of signaling (Le Borgne et al. 2005; Nichols et al. 2007) and, in the case of DLL4, signaling at a distance through the incorporation of DLL4 into exosomes (Sheldon et al. 2010; Sharghi-Namini et al. 2014). Adding further to the complexity is the extensive crosstalk between the Notch pathway and other major signaling networks such as receptor tyrosine kinase (RTK) signaling (Doroquez and Rebay 2006), WNT, hedgehog and transforming growth factor (TGF) β signaling (Borggrefe et al. 2016) janus kinase (JAK)/ signal transducer and activator of transcription (STAT) signaling (Josten et al. 2004) and hypoxia signaling (Gustafsson et al. 2005). To understand these mechanisms in greater depth, new studies are beginning to elucidate the role of the Notch ligands in this process. The five ligands share a similar overall architecture: Module at the N-terminus of Notch Ligands (MNNL) domains, a Delta/Serrate/Lag-2 (DSL) domain, between 6-14 EGF-like repeats, a transmembrane segment, and an intracellular domain (ICD) 100-150 amino acids in length. The extracellular moiety is essential for establishing the direct contacts with the Notch receptor necessary for eliciting Notch signaling (Luca et al. 2015). Biochemical and genetic evidence has shown that the intracellular domain is clearly essential for normal functioning of the full length protein (Heuss et al. 2008; Pintar et al. 2007; Six et

al. 2004; Ascano et al. 2002). Ligand ICDs harbour putative PDZ domains that couple them to membrane-bound proteins required for the maintenance of cell-cell junctions and likely play a central role in assembling those complexes necessary for ligand trafficking (Dejana 2004; Lee and Zheng 2010). Consistent with this, in Drosophila (Sun and Artavanis-Tsakonas 1996) and in vertebrates (Chitnis et al. 1995), Delta (and Serrate) ligands lacking an intracellular domain behave as dominant negative mutants such that the phenotypes resemble Notch or Delta loss-of-function mutants. Likewise, corruption of the DLL1 C-terminus has been shown to provoke mislocalization of the ligand (Heuss et al. 2008).

In common with the Notch receptor, the DLL1 and JAG ligands can be sequentially processed by proteases. Both ADAM (A Disintegrin And Metalloprotease) Metalloendopeptidases (Dyczynska et al. 2007; Six et al. 2003) and matrix metalloproteinase (MMP)14 (in the case of DLL1) (Jin et al. 2011) mediate ectodomain shedding by cleavage of the ligand close to the transmembrane domain on the extracellular side. Subsequent intramembrane processing by γ-secretase liberates the ICD (Ikeuchi and Sisodia 2003; LaVoie and Selkoe 2003). A growing body of evidence suggests that these ICDs might participate in signaling and downstream transcription and ectopically expressed ICDs have been localized to the nucleus (Liebler et al. 2012). Moreover, it has been reported that both DLL1 (Jung et al. 2011) and JAG1 ICDs (Kim et al. 2011) are able to bind to and to disrupt the function of the Notch ICD, by mediating its degradation in the case of the JAG ICD. The DLL1 ICD has also been pinpointed as a modulator of TGF-β/Activin signaling through binding to SMAD proteins (Hiratochi et al. 2007). A number of studies have described the effects of ligand ICDs at the cellular level. Inhibition of Notch1 signaling by the JAG1 ICD was shown to regulate cardiac homeostasis in the postnatal heart (Metrich et al. 2015). When ectopically expressed in mesenchymal stromal cells, the JAG1 ICD regulated haematopoietic stem and progenitor cell proliferation (Duryagina et al. 2013). Finally, overexpression of the DLL1 ICD brought about the growth arrest of primary endothelial cells (Kolev et al. 2005).

Collectively, the mechanisms described above determine the strength, the direction, the specificity and the nature of the output of the Notch signaling pathway. The emerging evidence that ICDs are biologically active is thus important for fully understanding Notch signaling in both normal and disease contexts, not least because the Notch pathway in general (Andersson and Lendahl 2014) and the DLL4 ligand in particular (Kuhnert et al. 2011; Sainson and Harris 2007) has emerged as a potential target for novel therapeutic interventions in cancer. The DLL4 ligand is integral to the development and homeostasis of numerous tissues, most notably the endothelium where it plays a central role in angiogenesis (Adams and Alitalo 2007; Herbert and Stainier 2011; Carmeliet and Jain 2011; Chung and Ferrara 2011; Geudens and Gerhardt 2011), hematopoiesis (Ayllón et al. 2015) and the intestinal crypt where it regulates maintenance of the stem cell compartment (Clevers 2013). To date

little is known about the function of the DLL4 intracellular domain. Here we provide evidence that the DLL4 ICD is needed for appropriate DLL4 sub-cellular localization. We show that it encodes a functional PDZ-binding domain which is necessary for associating to the MUPP1 scaffold protein. We further show that the DLL4 ICD is cleaved. The liberated DLL4 (and DLL1) ICD could interact with the bZIP domain of the JUN proto-oncogene thereby blocking it's binding to the consensus AP1 DNA-binding site. We found that JUN strongly stimulated endothelial cell sprouting which was inhibited by the ICDs of both DLL4 and DLL1. These data highlight a previously unreported role for JUN as a potent pro-angiogenic signal and the DLL4 ICD as a potential regulator of Notch signaling. Our evidence suggests that the ICDs of DLL4 (and DLL1) could control angiogenic sprouting by linking Notch signaling to the action of the AP-1 transcription factor complex.

RESULTS

The intracellular domain of DLL4 is cleaved

The amino acid sequence of the intracellular domain of DLL4 (hereafter referred to as DLL4INTRA) has been highly conserved throughout vertebrate evolution (Fig 1A). The four C-terminal amino acids (ATEV) encode a putative PDZ-binding domain (De Biasio et al. 2008). PDZ-binding domains have been shown to mediate protein-protein interactions, cell adhesion, tight junction integrity and trafficking (Lee and Zheng 2010) and loss of DLL4INTRA led to a complete disruption of normal DLL4 localization in primary human endothelial cells (Fig 1B). DLL4INTRA harbours a number of additional motifs that suggest it is functionally important including GSK consensus phosphorylation sites (which are utilized- ZF and DAB unpublished), a sumoylation motif and putative ubiquitination sites. Moreover, ectopically expressed DLL4INTRA is strongly enriched in the nucleus (Fig 1B) indicating that it may play a role independently of ensuring appropriate DLL4 sub-cellular distribution. To explore the function of this domain, we raised custom-made antibodies directed against epitopes unique to the C-terminus of human DLL4. Fig 1C shows that these antibodies recognized full length endogenous DLL4 as well as a number of smaller DLL4 species (predominant forms with masses between approximately 25-35 kDa and a lower molecular weight form of approximately 12 KDa). Similar sized fragments could be detected by Western blotting of lysates prepared from cells ectopically expressing full length DLL4 fused to a C-terminal HA epitope tag (Fig 1C). Through mass spectrometry, we determined that these fragments constitute the C-terminus of DLL4 (Fig 1C).

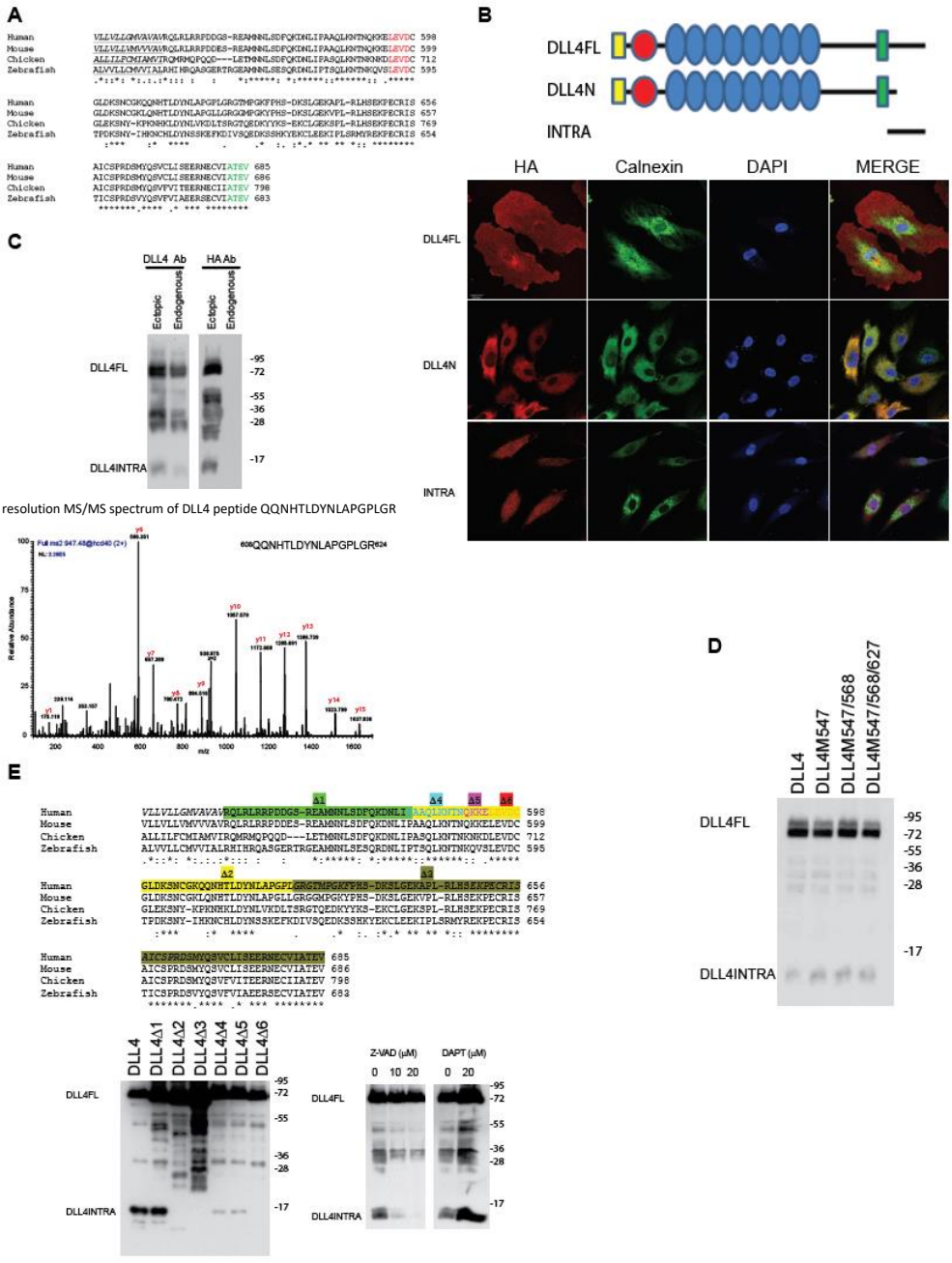

Figure 1. (A) The intracellular domain (ICD) of DLL4 is evolutionarily conserved. Highlighted are the transmembrane domain (underlined), a putative caspase cleavage site (red) and a PDZ-binding motif (green). (B) The DLL4 ICD is necessary for appropriate DLL4 sub-cellular localization and untethered DLL4INTRA is enriched in the nucleus. HUVECs were infected with lentiviruses for stably expressing the indicated HA epitope-tagged DLL4 constructs. DLL4N lacks the ICD and is otherwise identical to wild type DLL4. DLL4INTRA encompasses the ICD alone. The sub-cellular distribution of DLL4 was visualized by immunofluorescence using an HA antibody. Scale bar represents 20 μM.

< Figure 1 (continued). (C-E) The ICD of DLL4 is cleaved. (C) Mass spectrometry of cleaved DLL4 fragments. Endogenous DLL4 or DLL4 expressing a C-terminal HA epitope-tag were immunopurified from HUVECs. Samples were separated by SDS-PAGE and DLL4 ICDs were subjected to in-gel digestion with trypsin. Shown is an identified high resolution MS/MS spectrum of a recovered peptide corresponding to amino acids 608-624 of the DLL4 ICD. (D) The indicated ICD methionine residues of HA epitope tagged full length DLL4 were mutated to alanine. HA antibody Western blots were performed on lysates prepared from HUVECS stably expressing the indicated DLL4 ligands. (E) A conserved LEVD motif is required for cleavage of the DLL4 ICD. Left Panel: The indicated nested deletions of HA epitope tagged full length DLL4 were generated by site-directed mutagenesis. HA antibody Western blots were performed on lysates prepared from HUVECs stably expressing the indicated DLL4 ligands. Corresponding deletions are highlighted above. Right Panel: DLL4 ICD cleavage is blocked by the pan-caspase inhibitor, Z-VAD. Cells expressing wild type HA epitope tagged full length DLL4 were incubated overnight with or without the indicated concentrations of Z-VAD. DLL4 protein species were detected by HA antibody Western blotting.

The 25-35 KDa fragments are predicted to encompass the entire ICD, the transmembrane domain as well as sequences of the extracellular domain EGF repeats. The size of the shorter fragment indicates that it's composed uniquely of ICD sequences. Our evidence supports the view that this fragment is generated by post-translational proteolysis of the ICD distal to the transmembrane domain on the intracellular side. First, the molecular mass of the observed endogenous fragment precludes the possibility of it being generated by known mechanisms of alternative splicing alone. Second, mutation of the intracellular domain methionine residues failed to eliminate detection of the band in cells suggesting that it is not produced through use of internal initiation codons (Fig 1D). Third, a comprehensive deletion analysis mapped a putative cleavage site to the highly conserved LEVD motif (amino acids 594-597) (Fig 1E). LEVD closely resembles a consensus caspase cleavage site (Timmer and Salvesen 2007) and the pan-caspase inhibitor Z-VAD-FMK blocked the production of the DLL4ICD (Fig 1E). It has been reported that the closely related DLL1 ligand undergoes intramembrane processing mediated by γ-secretase to yield an intracellular fragment (Ikeuchi and Sisodia 2003; Six et al. 2003). Although we cannot formally rule out γ-secretase-dependent cleavage of DLL4, we found that release of the observed DLL4INTRA was not blocked by DAPT (data not shown). Together, these observations reveal two unique features of DLL4INTRA. They show that it is necessary for accurate ligand trafficking and also that it is proteolytically cleaved (and this proteolysis is caspase-dependent).

DLL4 interacts with the PDZ domain of MUPP1 and the bZIP domain of JUN

To investigate the potential molecular function(s) of the DLL4 intracellular domain, we performed yeast two-hybrid screens to identify partner proteins of DLL4INTRA. Three different DLL4 C-termini constructs were used as baits to independently screen a library prepared from primary HUVECs (Fig 2A).

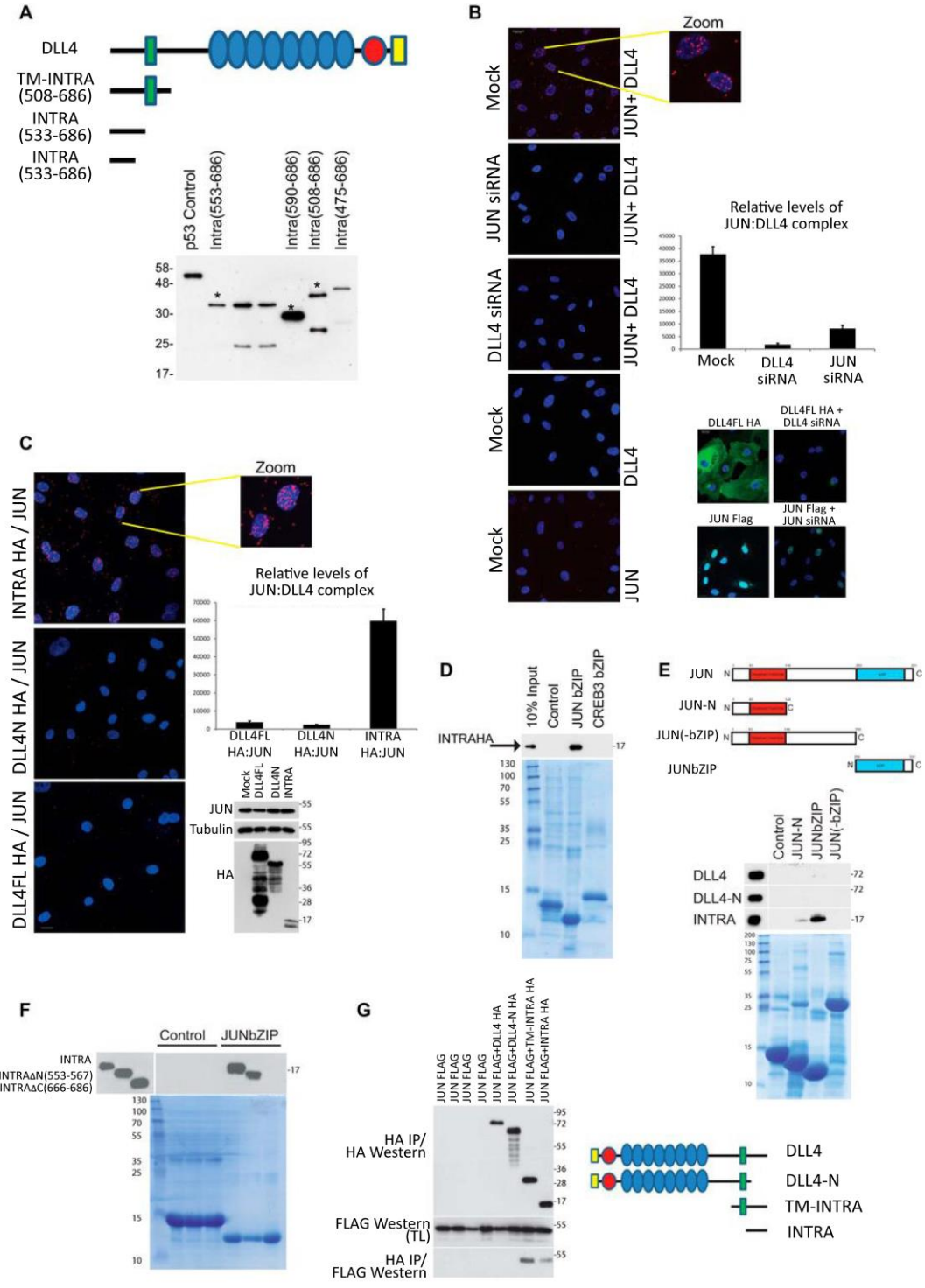
A
DLL4
TM-INTRA (508-686)
INTRA (533-686)
INTRA (533-686)
p53 Control
Intra(553-686)
Intra(590-686)
Intra(508-686)
Intra(475-686)
58-
48-
30-
25-
17-
B
Zoom
Mock
JUN+ DLL4
JUN siRNA
DLL4 siRNA
DLL4
JUN
Relative levels of JUN:DLL4 complex
Mock
DLL4 siRNA
JUN siRNA
DLL4FL HA
DLL4FL HA + DLL4 siRNA
JUN Flag
JUN Flag + JUN siRNA
C
Zoom
INTRA HA / JUN
DLL4N HA / JUN
DLL4FL HA / JUN
Relative levels of JUN:DLL4 complex
DLL4FL HA:JUN
DLL4N HA:JUN
INTRA HA:JUN
Mock
DLL4FL
DLL4N
INTRA
JUN
Tubulin
HA
D
10% Input
Control
JUN bZIP
CREB3 bZIP
INTRAHA
E
JUN
JUN-N
JUN(-bZIP)
JUNbZIP
Control
JUN-N
JUNbZIP
JUN(-bZIP)
DLL4
DLL4-N
INTRA
F
Control
JUNbZIP
INTRA
INTRAΔN(553-567)
INTRAΔC(666-686)
G
JUN FLAG
JUN FLAG
JUN FLAG
JUN FLAG
JUN FLAG+DLL4 HA
JUN FLAG+DLL4-N HA
JUN FLAG+TM-INTRA HA
JUN FLAG+INTRA HA
HA IP/ HA Western
FLAG Western (TL)
HA IP/ FLAG Western
DLL4
DLL4-N
TM-INTRA
INTRA

< Figure 2. **DLL4INTRA interacts with the bZIP domain of JUN.** (A) Yeast 2-hybrid baits were constructed by fusing DLL4 ICD fragments in-frame with a LexA DNA-binding domain either at the N- or the C-terminus of the ICD. Constructs were expressed in yeast to verify expression by Western blotting of lysates using a LexA antibody. A p53-LexA fusion is included as a control (Dualsystems Biotech). Predicted full length proteins of constructs used to screen a library prepared from HUVECs are marked with an asterisk. (B) A proximity ligation assay (PLA) revealed an endogenous DLL4:JUN complex. The graph shows relative complex formation per cell (right upper panel) that was abolished by ablation of either DLL4 or JUN (siRNA efficacies were demonstrated using cells ectopically expressing either DLL4 or JUN: see right lower panels). The endogenous DLL4:JUN complex was undetectable using single antibodies alone. Quantification was performed as described (see Methods) with an average of 100 cells scored. Scale bar represents 20 μM. (C) JUN specifically associated with the ICD of DLL4. PLA was performed on HUVECs ectopically expressing HA epitope tagged versions of either full length DLL4 (DLL4FL), the extracellular domain of DLL4, which lacks the ICD but retains the transmembrane domain (DLL4N) or the non-membrane tethered ICD of DLL4 (DLL4INTRA). Relative protein levels of DLL4 and endogenous JUN were determined by Western blotting with the indicated antibodies (right lower panel). The DLL4:JUN complex was detected using a combination of HA (for DLL4) and endogenous JUN antibodies. The graph shows relative complex formation per cell (right upper panel). Quantification was performed as described (see Methods) with an average of 100 cells scored. Scale bar represents 20 μM. (D and E) The ICD of DLL4 interacts biochemically with the bZIP domain of JUN. (D) Recombinant bZIP domains of JUN and CREB3 (and a control protein) were incubated with *in vitro* translated HA epitope-tagged DLL4INTRA. Recombinant proteins were visualized by Coomassie staining. Bound DLL4INTRA was detected by Western blotting. (E) Recombinant JUN domains (and a control protein) were incubated with *in vitro* translated HA epitope-tagged DLL4FL, DLL4N or DLL4INTRA. Recombinant proteins were visualized by Coomassie staining. Bound DLL4 was detected by Western blotting. (F) The C-terminus of DLL4INTRA is necessary for binding of DLL4INTRA to the JUN bZIP domain. Experiments were performed as in D and E. DLL4INTRAΔN lacks the N-terminal amino acids 553-567. DLL4INTRAΔC lacks the C-terminal amino acids 666-686. (G) The indicated constructs were stably expressed in HUVECs. JUN:DLL4 complexes were immunopurified from cell lysates using a rabbit HA polyclonal antibody and visualized by Western blotting with a Flag mouse monoclonal antibody. TM, transmembrane domain; IP, immunoprecipitation; TL, total lysate.

The PDZ domain-containing scaffold protein MUPP1 was obtained in all screens. It is involved in cell-cell junction integrity, including endothelial cell junctions, and protein trafficking (Balasubramanian et al. 2007; Dejana 2004). Immunoprecipitation studies in tissues culture cells corroborated the interaction between DLL4 and MUPP1 and its dependence on the extreme C-terminus (ATEV) of DLL4 lending substance to the view that DLL4INTRA has a bona fide PDZ-binding domain (Supplementary Fig 1; see Fig 1B). Less expected was the interaction with the bZIP-containing transcription factor JUN. We have previously established that JUN levels are dynamically balanced by VEGFR signaling in primary endothelial cells (Roukens et al. 2010) and several lines of evidence confirmed that DLL4INTRA and JUN can interact both *in vitro* and in cells. First, using a proximity ligation assay, we found that endogenous JUN and DLL4 associate (predominantly in the nucleus) in HUVECs (Fig 2B). By stably expressing engineered DLL4 mutants in HUVECs, we showed that DLL4INTRA was necessary and sufficient for this interaction (Fig 2C). Second, using purified

recombinant JUN protein domains and *in vitro* translated DLL4 proteins, we demonstrated that DLL4INTRA bound efficiently to the bZIP domain of JUN but not to the bZIP domain of CREB (Fig 2D). Third, Figs 2E and 2G substantiate our PLA findings (see Figs 2B and 2C) by showing that DLL4INTRA, but not the extracellular domain of DLL4 (DLL4N), is necessary for binding to JUN *in vitro* (Fig 2E) and in tissue culture cells (Fig 2G). Furthermore, the association between DLL4INTRA and JUN requires the bZIP domain of JUN (Fig 2E) as well as the highly conserved C-terminal twenty amino acids of DLL4, which are shared with the ICD of DLL1 (Fig 2F; See Supp. Fig 2), but not the PDZ-binding domain of DLL4INTRA (see Fig 3B). Collectively, these data highlight potentially a dual role for the DLL4ICD: it can interact with the bZIP domain of JUN and, in addition, it encodes a PDZ-binding domain that mediates a functional interaction with MUPP1.

DLL4INTRA blocks JUN binding to DNA

To determine the mechanistic consequences of DLL4INTRA:JUN binding, we established an *in vitro* assay to recapitulate JUN binding to DNA. For this, we employed a biotinylated consensus AP-1 DNA binding site and *in vitro* translated proteins. Fig 3A shows that JUN efficiently bound to the AP-1 site. As expected, JUN binding to the AP-1 site required the bZIP domain of JUN because a mutant lacking this domain, but not a mutant lacking amino acids C-terminal of this domain, was unable to bind the consensus sites, thus authenticating the specificity of the assay (Fig 3A). Compellingly, DLL4INTRA, but not DLL4N, impeded JUN associating to the AP-1 site (Fig 3B). Both the PDZ-binding motif of DLL4INTRA and sequences N-terminal of the LEVD motif were dispensable for this inhibition (Fig 3C). JUN represses or activates gene expression in a context-dependent fashion by docking on target promoters and through the differential recruitment of co-repressors and co-activators. To ascertain a more global view of regulation of JUN activity by DLL4INTRA, we performed transcriptome profiling of HUVECs ectopically expressing JUN in the presence or absence of DLL4INTRA or DLL4N. Ectopic expression of JUN is highly pro-angiogenic (see Fig 4) and leads to a dramatic alteration in the set of expressed genes (Fig 3D: compare Mock and JUN). Whereas co-expression of DLL4N had relatively more modest effects on the JUN-controlled transcriptome, DLLINTRA significantly altered the expression pattern of JUN-controlled genes (Fig 3D). These findings were verified by real time quantitative PCR (qPCR) of a subset of the genes, including DLL4 (Fig 3E). To test if these effects could have resulted from DLL4INTRA directly occluding JUN DNA-binding, we investigated JUN recruitment to the proximal promoter of DLL4. We have previously shown that DLL4 expression (and JUN expression) is highly attuned to VEGFR signaling in HUVECs (Roukens et al. 2010). Fig 3F shows that short-hairpin (sh) RNA-mediated loss of JUN in HUVECs abrogated the VEGF-stimulated wave of DLL4 expression signifying that DLL4 expression is governed by JUN.

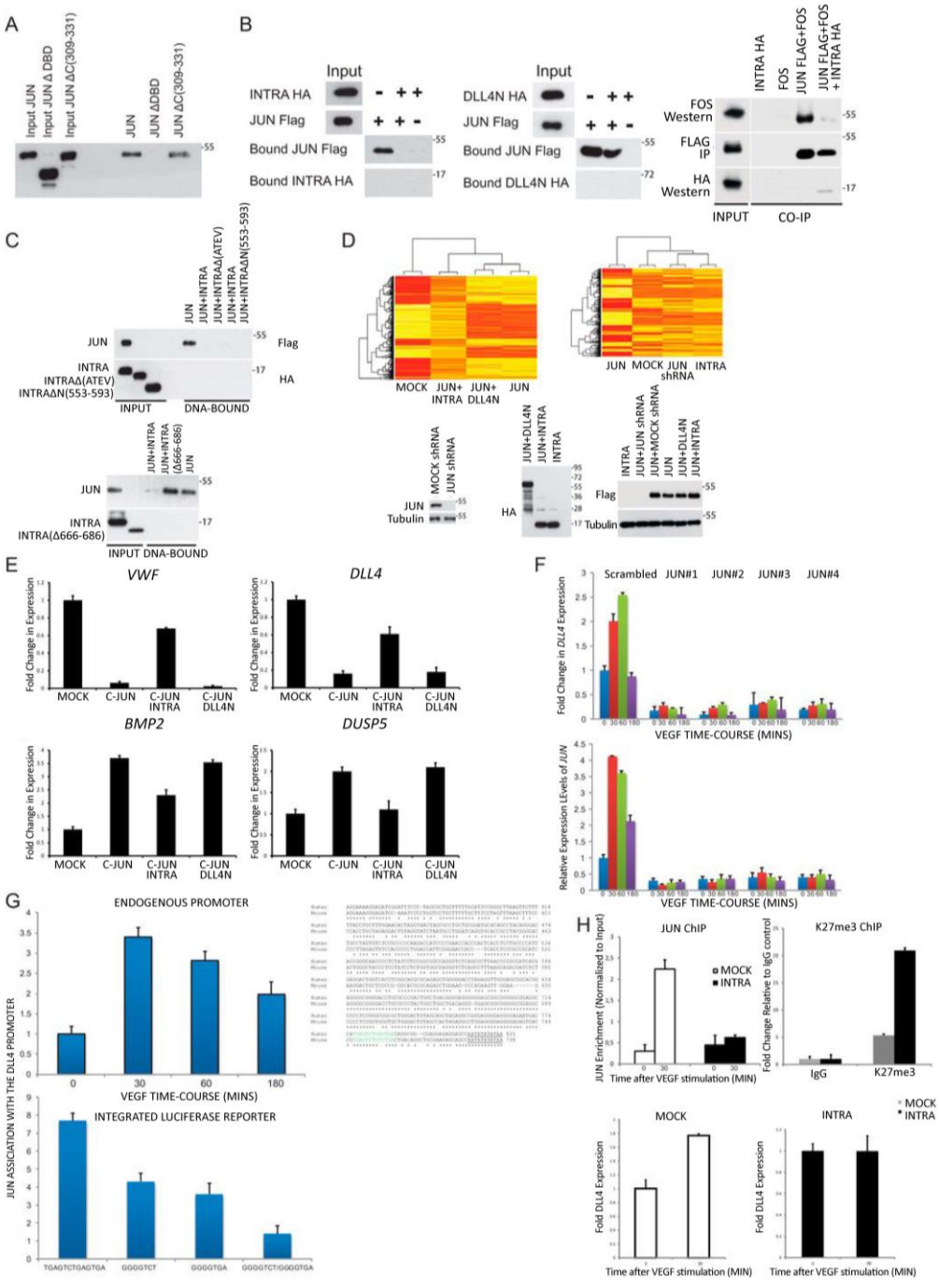
A
Input JUN
Input JUN Δ DBD
Input JUN ΔC(309-331)
JUN
JUN ΔDBD
JUN ΔC(309-331)
B
Input
INTRA HA
JUN Flag
Bound JUN Flag
Bound INTRA HA
DLL4N HA
FOS Western
FLAG IP
HA Western
INTRA HA
FOS
JUN FLAG+FOS
JUN FLAG+FOS + INTRA HA
INPUT
CO-IP
C
JUN
JUN+INTRA
JUN+INTRAΔ(ATEV)
JUN+INTRA ΔN(553-593)
INTRA
INTRAΔ(ATEV)
INTRAΔN(553-593)
Flag
HA
INPUT
DNA-BOUND
JUN+INTRA (Δ666-686)
INTRA(Δ666-686)
D
MOCK
JUN+ INTRA
JUN+ DLL4N
JUN
JUN MOCK JUN shRNA INTRA
MOCK shRNA
JUN shRNA
JUN
Tubulin
JUN+DLL4N
JUN+INTRA
INTRA
HA
INTRA
JUN+JUN shRNA
JUN+MOCK shRNA
JUN
JUN+DLL4N
JUN+INTRA
Flag
Tubulin
E
VWF
DLL4
BMP2
DUSP5
Fold Change in Expression
MOCK
C-JUN
C-JUN INTRA
C-JUN DLL4N
F
Scrambled
JUN#1
JUN#2
JUN#3
JUN#4
Fold Change in DLL4 Expression
VEGF TIME-COURSE (MINS)
Relative Expression LEvels of JUN
G
ENDOGENOUS PROMOTER
VEGF TIME-COURSE (MINS)
JUN ASSOCIATION WITH THE DLL4 PROMOTER
INTEGRATED LUCIFERASE REPORTER
TGAGTCTGAGTGA
GGGGTCT
GGGGTGA
GGGGTCTGGGGTGA
H
JUN ChIP
MOCK
INTRA
JUN Enrichment (Normalized to Input)
Time after VEGF stimulation (MIN)
K27me3 ChIP
Fold Change Relative to IgG control
IgG
K27me3
MOCK
INTRA
Fold DLL4 Expression
Time after VEGF stimulation (MIN)

< Figure 3. **DLL4INTRA antagonizes JUN DNA-binding.** (A) JUN binds to a consensus AP-1 DNA binding site *in vitro*. A biotinylated double-stranded oligonucleotide harboring three consensus AP-1 binding sites was incubated with the indicated Flag epitope tagged *in vitro* translated proteins. JUNΔDBD lacks the DNA-binding domain. JUNΔC(309-331) lacks the C-terminal amino acids abutting the DNA-binding domain. DNA-bound JUN was detected by Western blotting. (B) DLL4INTRA impedes JUN binding to DNA. As in (A), AP-1 DNA binding sites were incubated with the indicated *in vitro* translated proteins. DNA-bound JUN was detected by Western blotting. (C) The putative PDZ-binding motif of DLL4INTRA is dispensable for DLL4INTRA binding to JUN. As in (A and B), AP-1 DNA binding sites were incubated with the indicated *in vitro* translated proteins. INTRAΔ(ATEV) lacks the putative C-terminal PDZ-binding motif. INTRAΔN(553-593) lacks the highlighted N-terminal amino acids. DNA-bound JUN was detected by Western blotting. (D) DLL4INTRA alters the JUN-controlled transcriptome. A microarray analysis was performed on HUVECs stably expressing the indicated constructs. Protein levels were determined by Western blotting with the indicated antibodies (Lower panel). Heat maps show a comparison of global gene expression profiles (Upper panels). (E) Expression levels in HUVECs of the indicated transcripts were determined by real-time qPCR. All values were averaged relative to TATA binding protein (TBP), signal recognition particle receptor (SRPR) and calcium-activated neutral proteinase 1 (CAPNS1). Values were normalized against Mock treated cells. Values represent +/- the standard deviation (n = 3). (F) JUN controls DLL4 expression. Real time qPCR was performed on cDNA prepared from cells stably infected with one of four different JUN shRNA constructs and stimulated with or without VEGF for the shown time course (minutes). All values were averaged relative to TATA binding protein (TBP), signal recognition particle receptor (SRPR) and calcium-activated neutral proteinase 1 (CAPNS1). Values were normalized against the time 0 time point of Mock infected cells. Values represent +/- the standard deviation (n = 3). (G-H) JUN associates with the proximal promoter of human DLL4. (G) Upper panel: A ChIP analysis was performed on HUVECs incubated with or without 50 ng/ml VEGF for the indicated times. Three different primer sets centered on the illustrated promoter region were used and a single representative is shown (all three gave very similar results). Equivalent amounts of rabbit IgG were used as a control and results are presented as fold changes in recovery (as a fraction of input) relative to the 0 time point. Lower panel: Expression of a stably integrated luciferase reporter was placed under the control of the depicted wild type DLL4 proximal promoter or the same promoter in which the putative AP-1 sites have been singly or doubly mutated. The alignment of the human and mouse DLL4 promoter regions highlights the presumed transcription start site (underlined). Conserved consensus AP-1 DNA-binding sites are shown in green. A ChIP analysis was performed on reporter-expressing HUVECs incubated for 30 minutes with 50 ng/ml VEGF. Equivalent amounts of rabbit IgG were used as a control and results are presented as fold changes in recovery (as a fraction of input) relative to the control IgG. Two different primer sets were centered on the integrated luciferase gene. A single representative is shown (both gave comparable results). (H) Upper graphs: ChIP analyses were performed with the indicated antibodies (as described in G) on control HUVECs and HUVECs stably expressing DLL4INTRA. Lower graphs: DLL4 expression levels in control HUVECs and HUVECs stably expressing DLL4INTRA were determined by real-time qPCR. All values were averaged relative to TATA binding protein (TBP), signal recognition particle receptor (SRPR) and calcium-activated neutral proteinase 1 (CAPNS1). Values were normalized against Mock treated cells. Values represent +/- the standard deviation (n = 3). IP, immunoprecipitation; VWF, von Willebrand factor. Error bars represent S.D.

In support of this view, we found that endogenous JUN associated with the proximal promoter of DLL4 and, using an integrated luciferase reporter, loss of a consensus AP-1 site upstream of the DLL4 TATA box significantly diminished the detectable levels of promoter-bound JUN (Fig 3G). Accordantly, ectopic expression of DLLINTRA inhibited VEGF-dependent association of JUN with the

DLL4 promoter (Fig 3H, upper graph) and led to a concomitant inhibition of VEGF-stimulated DLL4 expression (Fig 3H, lower graphs). Consistent with these findings, stable expression of DLL4INTRA augmented the levels of the repressive H3K27me chromatin methylation mark found at the DLL4 proximal promoter (Fig 3H, upper graph). These data indicate that DLL4INTRA can negatively regulate JUN binding to DNA and, in consequence, control expression of genes required for endothelial sprouting.

DLL4INTRA attenuates JUN-mediated endothelial cell sprouting

To elucidate the biological consequences of DLL4INTRA binding to JUN, we used a 3D-matrigel sprouting assay. Figure 4A shows that enhanced JUN levels hugely increased endothelial sprouting (including filopodia formation), whereas loss of endogenous JUN abolished the ability of HUVECs to sprout. JUN-stimulated sprouting depended on the bZIP domain of JUN, and thus presumably relies on JUN binding to DNA, because a JUN mutant lacking this domain acted as a dominant negative resulting in strong inhibition of sprouting (Fig 4A). In this assay, wild type sprouting networks are relatively short-lived and collapse after approximately 24 hours. By contrast, endothelial cells ectopically expressing JUN were robustly sustained and continued to sprout for several weeks. Additionally, these JUN expressing cells could sprout efficiently in the absence of exogenous VEGF (ZF and DB, unpublished). In agreement with our prior findings that DLL4INTRA obstructs JUN DNA-binding (see Fig 3), Fig 4B shows co-expression of DLL4INTRA, but not DLL4N, restricted JUN-driven endothelial sprouting.
AP-1 transcription factors are characterized by the conserved bZIP domain, which mediates homo- and heterodimerization of AP-1 family members and DNA binding. This begs the question as to whether DLL4INTRA might also influence the activity of other AP-1 family members such as JUNB, which has an established role in vascular morphogenesis. Our experiments show that JUNB, like JUN, strongly stimulated endothelial tube formation (Fig. 5A), and DLL4INTRA could inhibit this process (Fig. 5B).

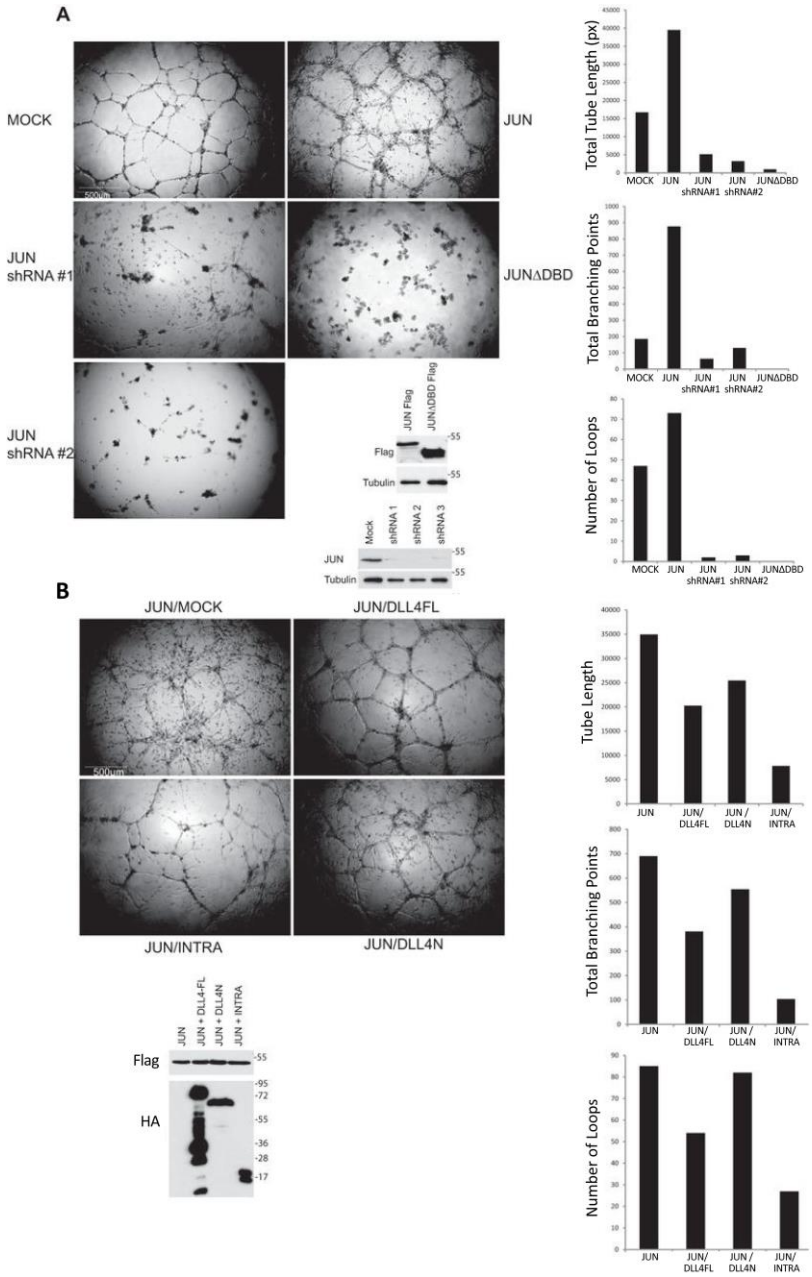

Figure 4. (A) JUN strongly stimulates endothelial cell tube formation/sprouting. HUVECs lacking endogenous JUN or ectopically expressing the indicated JUN proteins were cultured in Matrigel in the presence of 50 ng/ml VEGF. A representative of several independent experiments is shown. After 24 h, in-house computer software was used to quantify the total length of the sprouts, the number of branch points, and the number of loops. Protein levels were determined by Western blotting with the indicated antibodies. Scale bar, 500 µm. (B) DLL4INTRA attenuates JUN-mediated sprouting. HUVECs ectopically expressing the indicated proteins were cultured in Matrigel in the presence of 50 ng/ml VEGF. Experiments were conducted and quantified as in A. Scale bar,500 µm. DBD, DNA-binding domain; DLL4FL, full-length DLL4.

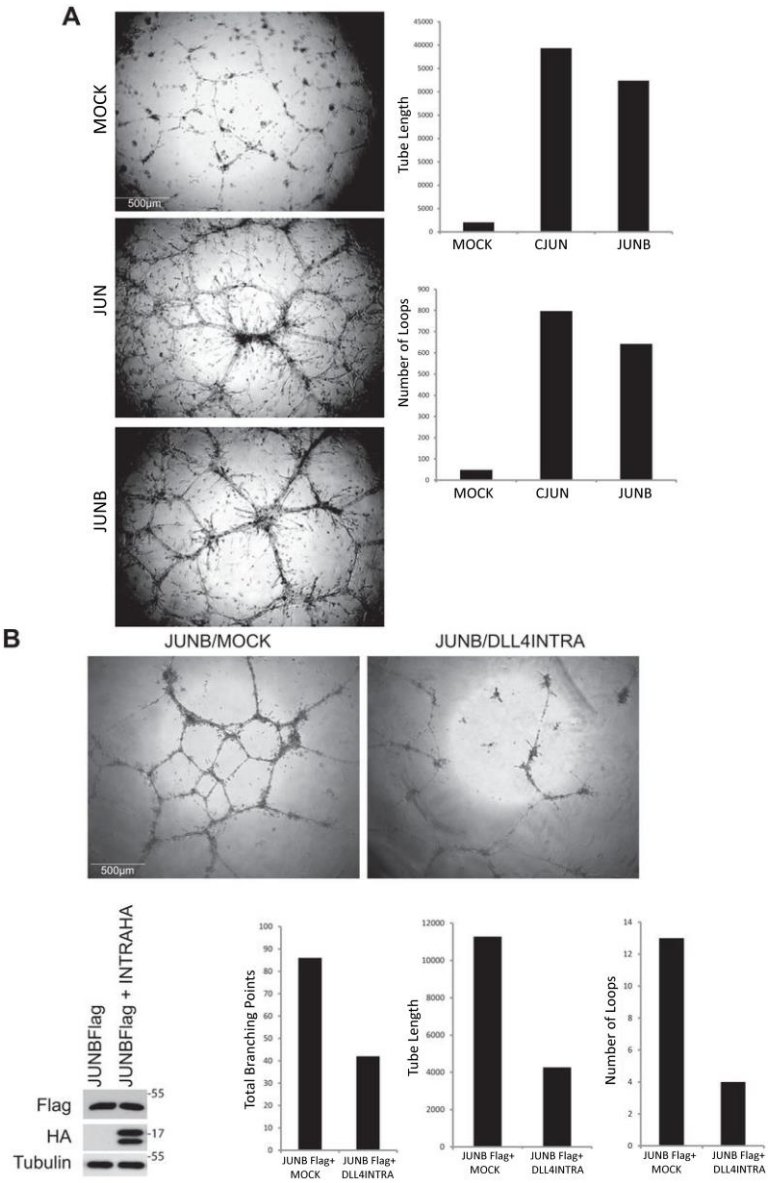

Figure 5. (A) JUNB strongly stimulates endothelial cell tube formation/sprouting. HUVECs ectopically expressing JUN or JUNB were cultured in Matrigel in the presence of 50 ng/ml VEGF. A representative of several independent experiments is shown. After 48 h, in-house computer software was used to quantify the total length of the sprouts, the number of branch points, and the number of loops. Protein levels were determined by Western blotting with the indicated antibodies. Scale bar, 500 m. B, DLL4INTRA attenuates JUNB-mediated sprouting. HUVECs ectopically expressing the indicated proteins were cultured in Matrigel in the presence of 50 ng/ml VEGF. A representative of several independent experiments is shown. After 24 h, in-house computer software was used to quantify the total length of the sprouts, the number of branch points, and the number of loops. Protein levels were determined by Western blotting with the indicated antibodies. Scale bar, 500 m.

DISCUSSION

In this study, we have presented evidence that the intracellular domain (ICD) of DLL4 (DLL4INTRA) could perform a dual function: it is essential for establishing normal DLL4 sub-cellular localization and, strikingly, the untethered ICD interacted with and inhibited the activity of the JUN transcription factor. By means of chemical inhibitors and targeted mutagenesis we demonstrated that one mechanism of ICD cleavage is caspase-dependent (see Fig 1). The pattern of cellular DLL4 protein species indicates that multiple DLL4 cleavage events could occur but their precise nature are yet to be delineated. What triggers the cleavage event(s), or if proteolysis is constitutive, is also currently unclear and will be important to establish. Certainly, DLL4INTRA is highly conserved and harbors a number of motifs that might control its function (see Introduction) and which could influence its fate. We found that endogenous DLL4INTRA accumulated following incubation of cells with VEGF (Supplementary Fig 2). Future work will determine if this simply reflects increased levels of DLL4 and/or specific signaling events. Related to this, unravelling the mechanism(s) of DLL4INTRA turnover could shed further light on its function. It has been noted that the DLL4 ICD contains an intrinsically disordered region (IDR) terminating in a structured C-terminal PDZ-binding domain (De Biasio et al. 2008). This conformation resembles the proto-oncogene FOS (Campbell et al. 2000; Gomard wt al. 2008; van Ijzendoorn et al) and other signaling proteins and transcription factors (Erales and Coffino 2014). We recently found that the C-terminus of FOS is composed of a comparable IDR/structured extreme C-terminus which controls intrinsic, rapid proteasomal degradation of FOS and a similar mechanism might control the activity of DLL4INTRA (van Ijzendoorn et al.). Indeed, we found that DLL4INTRA protein levels are strongly stabilized when the proteasome is blocked by MG132 indicating that DLL4INTRA is rapidly turned over (ZF and DAB, unpublished).

JUN is a member of the AP-1 family of transcription factors which plays a pivotal role in cell growth, differentiation and survival as well as the DNA damage response (Shaulian and Karin 2001; Shaulian and Karin 2002). These transcription factors are characterized by a conserved bZIP domain which begs the question as to whether DLL4INTRA might also influence the activity of other AP-1 family members such as JUNB which has an established role in vascular morphogenesis (Licht et al. 2006; Kanno et al. 2012; Schorpp-Kistner et al. 1999). Our experiments show that JUNB, like JUN, strongly stimulated endothelial cell sprouting (Supplementary Fig 3A) and DLL4INTRA could inhibit JUNB-driven endothelial cell sprouting (Supplementary Fig 3B). A related question is whether other Notch ligand ICDs can function similarly to DLL4INTRA. The DLL1 ligand shares a high degree of amino acid identity with DLL4 including approximately 40% of the ICD (see Supplementary Fig 4). Our results suggest that DLL1INTRA,

like DLL4INTRA, can bind to the bZIP domain of JUN (Supplementary Fig 4A) and block JUN binding to a consensus AP-1 DNA site (Supplementary Fig 4B). Interestingly, unlike DLL4INTRA, DLL1INTRA could also interact with the bZIP domain of CREB3 *in vitro* (see Supplementary Fig 4A) raising the possibility that they have specific as well as overlapping activities. At the cellular level, DLL1INTRA, in common with DLL4INTRA, inhibited JUN-driven endothelial cell sprouting (Supplementary Fig 4C). Collectively, these results highlight a potential link between untethered Notch ligand ICDs and the immediate-early gene, AP-1 transcription factor complex. Genome-wide screens have established the importance of ETS and AP-1 transcription factor cooperation by their associating to neighbouring AP-1 and ETS DNA-binding sites (Plotnik et al. 2014). Since ETS transcription factors are essential for angiogenesis (Roukens et al. 2010; Craig and Sumanas 2016; Randi et al. 2009) and have been reported to control DLL4 expression (Roukens et al. 2010; Shah et al. 2017) it is noteworthy that JUN potently stimulates endothelial sprouting and is required for normal expression of DLL4 (see Fig 3). JUN/DLL4INTRA interactions, therefore, could form part of a feedback loop whereby VEGF-dependent changes in DLL4 expression (as well as other angiogenesis-regulating genes) depend on ETS/AP-1 factors and are regulated by DLL ICDs.

In summary, our data lend support to the idea that biologically active Notch ligand ICDs could help establish appropriate endothelial cell responses through crosstalk with AP-1-dependent signal transduction pathways. They further highlight the possibility that corruption of this mechanism might play a role in disease processes such as tumor angiogenesis and developmental disorders. This is important because the Notch pathway has emerged as primary target for the design of novel therapeutic interventions in cancer (Andersson and Lendahl 2014). Also, it has recently been reported that heterozygous loss-of-function DLL4 mutations are a potential cause of Adams-Oliver syndrome, a rare congenital disorder characterized by multiple defects including vascular and cardiac anomalies (Meester et al. 2015). Two of the identified DLL4 mutations are nonsense mutations that would be predicted to lead to complete loss of the DLL4 ICD.

EXPREMENTAL PROCEDURE

Yeast Two-hybrid Screens

Screens were performed according to the manufacturer's protocol (Dualsystems Biotech). Bait and prey were rescued from yeast colonies and genuine interactions were confirmed through re-transfection of yeast. Protein-protein interactions were tested quantitatively using a LacZ reporter assay (Dualsystems Biotech).

Proximity Ligation Assay

Proximity Ligation Assay was performed using a Duolink in situ PLA kit (Sigma) according to the manufacturer's protocol. For each condition, an average of 100 cells were scored. Error bars show the standard error of the mean. Statistical analysis of fluorescent signal was performed by using Blobfinder (http://www.cb.uu.se/~amin/BlobFinder/).

Mass Spectrometry

Endogenous DLL4 or HA epitope tagged DLL4 were immunopurified from duplicate lysates each prepared by lysing HUVECS (20 x 15 cm and 10 x 15 cm dishes respectively) in ice-cold lysis buffer (50 mM Tris, pH 7.5, 1% NP40, 0.1% SDS, 0.5% Na-deoxycholate, 150 mM NaCl). Protein bands were excised from SDS-PAGE gels and subjected to in-gel trypsin digestion.

Cell culture, biochemistry and molecular biology

Primary HUVECs (Lonza) were cultured in EGM2 medium (Lonza). Human embryonic kidney 293T cells were cultured in DMEM (Gibco) supplemented with 10% fetal bovine serum (Gibco). 293T cells were typed using short tandem repeat analysis of the DNA and all cell lines were checked for mycoplasma with the MycoAlert kit (Lonza). Transfections, lentivirus production and cell infections, Western blotting and co-immunoprecipitations have been described previously (Roukens et al. 2008). All lysis buffers contained a cocktail of protease inhibitors (phenylmethylsulfonyl fluoride, trypsin inhibitor, pepstatin A, leupeptin, aprotinin).

Recombinant protein production/ *in vitro* protein:protein interaction

Domains for recombinant protein production were cloned into the pET 28a vector in-frame to an N-terminal 6x HIS epitope. His epitope–tagged proteins were manufactured in Escherichia coli BL21(DE3). Following sonication (Misonix Sonicator 3000) in 3 mls ice-cold buffer / 50 ml bacterial culture (150 mM NaCl, 2.7 mM KCl, Na2HPO4, KH2PO4, 20 mM imidazole, 10 mM □-mercaptoethanol), proteins were purified onto 50 ul of Nickel- agarose beads (Qiagen) by 3 hours rolling at 4C. Beads were washed in 10 x 1 ml of the same buffer. Protein yields were determined by Bradford assay (Bio-Rad) and relative protein integrity and purity was determined by SDS-PAGE and Colloidal Blue staining (Invitrogen). 5-10 µl of HIS beads (purified recombinant protein) in 1 ml of buffer were incubated for 2 hours at 4oC with *in vitro* translated DLL4 proteins made using the TNT-coupled reticulocyte *in vitro* translation system (Promega). Beads were washed x10 with 1 ml of buffer. Proteins were separated by SDS-PAGE and associated proteins were detected by Western blot.

Plasmid and shRNA construction

Unless otherwise stated, all cDNAs were fused in-frame with a Flag or an HA epitope tag and were cloned into the pLV lentiviral vector and pCS2 expression plasmid. The luciferase reporter was constructed by cloning 1 kb of the DLL4 proximal promoter downstream of the luciferase gene in the pLV lentiviral vector. All mutants were engineered by site-directed mutagenesis using Phusion High-Fidelity DNA polymerase (Thermofisher). All constructs were verified by Sanger sequencing (Macrogen). The following Mission shRNA library clones (Sigma) were used:

shRNA TRCN0000010366 JUN
shRNA TRCN0000039589 JUN
shRNA TRCN0000009845 JUN
shRNA TRCN0000039588 JUN
shRNA TRCN0000039590 JUN
shRNA TRCN0000039591 JUN
shRNA TRCN0000039592 JUN
shRNA TRCN0000033414 DLL4
shRNA TRCN0000033415 DLL4
shRNA TRCN0000033416 DLL4
shRNA TRCN0000033417 DLL4
shRNA TRCN0000033418 DLL4

The following siRNA duplexes (Thermo Scientific) were used (sense strands are shown):

DLL4 siRNA 1: GCUCCACUGCGAGAAGAAU
DLL4 siRNA 2: GCAUGGUGGCAGUGGCUGUUU
JUN siRNA 1: GGAUCAAGGCGGAGAGGAAUU
Scrambled: ON-TARGET plus Non-targeting siRNA (D-001810-01-05)

HUVECs cells were transfected with duplexes using DharmaFECT transfection reagent according to the manufacturer's recommendations (Thermo Scientific). Transfected cells were incubated for 72-hours prior to PLA assays. Efficient delivery of siRNA and subsequent silencing were tested by immunostaining and Western blotting.

Transcriptome Profiling
Total RNA was isolated using Trizol (Invitrogen) and further purified using RNeasy Minikit (Qiagen). Total RNA was labeled using Illumina RNA Amplification kit (Ambion). Duplicate samples from two independent experiments were tested. Gene profiles were determined by hybridization to Sentrix HumanHT-12 Expression Beadchips (ServiceXS). Microarray data has been posted on GEO database.

Analysis of mRNA expression
RNA isolation, first strand cDNA synthesis and analysis of expression of transcripts by quantitative PCR were performed as previously described 35. The following primer sets were used (5' to 3' orientation):
DLL4FOR ccctggcaatgtacttgtgat
DLL4REV tggtgggtgcagtagttgag
JUNFOR cgcctgataatccagtcca
JUNREV ttcttggggcacaggaact
DUSP5FOR caaatggatccctgtggaa
DUSP5REV ccctttccctgacacagtc
VWFFOR gtgcagacccaacttcacct
VWFREV gggtggggacactcttttg
BMP2FOR cagaccaccggttggaga
BMP2REV ccactcgtttctggtagttcttc

All qPCR values were averaged relative to the control gene, TATA binding protein (TBP), signal recognition particle receptor (SRPR) and calcium-activated neutral proteinase 1 (CAPNS1). For each data point, PCRs were performed in triplicate and error bars show standard deviations from the mean.

HUVEC sprouting assay
96-well plates were coated with 60 µl of Matrigel/well 30 minutes prior to seeding HUVECs. EGM-2 medium was supplemented with 50 ng/ml recombinant human VEGF 165 (R and D Systems). Images were taken at multiple timepoints. Analysis of the sprouting was performed with Stacks (In-house software: LUMC, MCB).

Immunofluorescence
Immunostaining was performed as previously described (Roukens et al. 2008) using Alexa Fluor 488 goat anti-mouse secondary antibodies (Thermo Fisher scientific). Imaging was performed with a Leica SP8 confocal microscope.

Protein-DNA interaction assays

In vitro translated protein was made using the TNT-coupled reticulocyte *in vitro* translation system (Promega). 50 pmol biotinylated double-stranded oligonucleotides harbouring three contiguous AP-1 DNA-binding sites were coupled to MyOne Streptavidin C1 beads (Invitrogen). Reactions were incubated at 4°C with vigorous shaking for 30 minutes in the presence of 1 µg poly (dI/dC), 4 mM Spermidine, 50 mM KCl, 10 mM HEPES (pH 7.6), 5 mM MgCl2, 10 mM Tris pH 8, 0.05 mM EDTA (pH 8), 0.05 mM, 0.1% Triton X-100 and 20% glycerol. Beads were successively washed three times with the aforementioned buffer. Associated proteins were eluted in Laemmli buffer and protein-DNA interactions were determined by Western blotting.

ChIP

Confluent 10 cm tissue culture dishes of HUVECs were cross-linked for 10 minutes with formaldehyde (final concentration = 1%). Glycine was added to a final concentration of 0.125 M and incubated for 5 minutes. Cells were washed 2x with PBS and subsequently lysed in ChIP Lysis Buffer (1%SDS,10 mM EDTA, 50mM Tris-HCL pH 8.1) supplemented with protease inhibitors. Chromatin was sheared by sonication (Bioruptor UCD-200 ultrasound sonicator: Diagenode), resulting in DNA fragments between 500 and 1000 bp in size. After centrifugation, 10% of the sample was kept as Input. Chromatin was diluted 10x in dilution buffer (1%Triton X-100, 2mM EDTA pH 8.0, 150 mM NaCl, 20 mM Tris-HCl pH 8.1 supplemented with protease inhibitors). For immunoprecipitation, 2 µg of test or control antibody was added to the diluted chromatin and incubated overnight at 4°C. Blocked protein A-Sepharose beads (10µg of sonicated herring sperm DNA) were added for 2 hrs. Beads were extensively washed (0.1 % SDS, 0.1% NaDOC, 1% TritonX-100, 0.15 M NaCl, 1mM EDTA, 0.5 mM EGTA, 20 mM HEPES) and complexes were eluted with elution buffer (1% SDS, 0.1 M NaH2CO3, 0.2 M NaCl) at 65oC overnight to reverse crosslinking. Associated DNA was purified by phenol/chloroform extraction and ethanol precipitation (in the presence of 15 µg/ml glycogen (Roche)). Realtime qPCR was used to determine recovery of specific DNA fragments. The following primers were used (5' to 3' orientation):

DLL4promFOR A ttctttttacctgctttggaaca
DLL4promREV A agtccctgtaggctgtgcat
DLL4promFOR B aatgaccatgagtctgagtgaca
DLL4promREV B cgccgctactgaaacctg
DLL4promFOR C gggtgggcactcataggtt
DLL4promREV C aaaccagcgctagggaaatc
DLL4promFOR D tcaggagagttcctccttgc
DLL4promREV D tgagtccagcttcagttcctg
DLL4promFOR E acgctcccaacctcttgtt

DLL4promREV E ccgagcatggtctgattttt
DLL4promFRO F tcatgaatgtcttttgatgctga
DLL4promREV F tcccagagatctagaaaggctct
DLL4promFOR G gaacacgaggccaagagc
DLL4promREV G cgcgtcttctgtctaatcctg
LuciferaseFOR 1 catgaccgagaaggagatcg
LuciferaseREV 1 cagcttcttggcggttgta
LuciferaseFOR 2 tgagtacttcgaaatgtccgttc
LuciferaseREV 2 gtattcagcccatatcgtttcat

Antibodies and drugs

Antibodies were obtained from the following sources: custom-made rabbit and goat polyclonals were generated by Eurogentec; Flag mouse M2 monoclonal (Sigma-Aldrich); anti-HA.11 mouse monoclonal (Covance); anti- Ha rabbit polyclonal (Abcam); anti-JUN rabbit (Cell Signaling Technology); anti-JUN mouse (Santa Cruz); anti-Flag rabbit (Sigma); anti-γTubulin (Sigma); H3K27me3 (Bethyl Laboratories). Z-VAD was purchased from Sigma.

ACKNOWLEDGMENTS

We thank members of the Departments of Molecular Cell Biology for helpful discussions, technical advice and support in particular Professor Peter ten Dijke. We are very grateful to Dr. Jan Oosting for the analyses of the microarray data and Annelies van der Laan for help with the confocal microscopy. We are indebted to Dr. Hans Vrolijk for designing computer software for quantifying sprouting assays. This work was supported by the Dutch Cancer Society to DAB (30861).

AUTHOR CONTRIBUTIONS

ZF and FR performed the majority of experiments assisted by DAB. AL and JVO performed mass spectrometry analyses. DAB supervised the study and wrote the paper. All authors read and approved the paper.

REFERENCES

1. Adams, R.H and Alitalo, K. (2007). Molecular regulation of angiogenesis and lymphangiogenesis. Nar Rev Mol Cell Biol 8(6), 464-78.

2. Andersson, AR and Lendahl, U. (2014). Therapeutic modulation of Notch signaling- are we there yet? Nature Rev. Drug Discovery 13, 357-378.

3. Ascano, JM; Beverly, LJ and Capobianco, AJ. (2002). The C-terminal PDZ-ligand of JAGGED1 is essential for cellular transformation. J Biol Chem. 278(10), 8771-9.

4. Aster, JC; Pear, WS and Blacklow SC. (2017). The varied roles of Notch in cancer. Annu. Rev. Pathol. Mech. Dis. 12, 245-75.

5. Ayllón, V; Bueno, C; Ramos-Mejía, V; Navarro-Montero, O; Prieto, C; Real, PJ; Romero, T; García-León, MJ; Toribio, ML; Bigas, A; and Menendez, P. (2015). The Notch ligand DLL4 specifically marks human hematoendothelial progenitors and regulates their hematopoietic fate. Leukemia 29, 1741-1753.

6. Balasubramanian, S; Fam, SR and Hall, RA. (2007). GABAB Receptor Association with the PDZ Scaffold Mupp1 Alters Receptor Stability and Function. J Biol Chem 282(6), 4162-4171.

7. Borggrefe, T; Lauth, M, Zwijsen, A; Huylebroeck, D; Oswald, F and Giaimo, BD. (2016). The Notch intracellular domain integrates signals from Wnt, Hedgehog, TGF/BMP and hypoxia pathways. BBA- Molecular Cell Research 1863 (2), 303-313.

8. Braune, EB and Lendahl, U. (2016) Notch- a Goldilocks signaling pathway in disease and cancer therapy. Discov Med 21(115), 189-196.

9. Bray, SJ. (2016) Notch Signaling in context. Nature Rev. Mol. Cell Biol. 17, 722-735.

10. Bray, SJ. (2006). Notch signaling: a simple pathway becomes complex. Nature Rev. Mol. Cell Biol. 7, 678-689.

11. Campbell, K.M; Terrell, A.R; Laybourn, P.J and Lumb K.J. (2000). Intrinsic structural disorder of the C-terminal activation domain from the bZIP transcription factor Fos. Biochemistry 39, 2708-2713.

12. Carmeliet, P and Jain, RK. (2011). Molecular mechanisms and clinical applications of angiogenesis. Nature 473, 298-307.

13. Chitnis, A; Henrique D; Lewis, J, Ish-Horowicz, D and Kintner, C. (1995). Primary neurogenesis in Xenopus embryos regulated by a homologue of the Drosophila neurogenic gene Delta. Nature 376, 761-766.

14. Chung, AS and Ferrara, N. (2011). Developmental and pathological angiogenesis. Annu. Rev. Cell Dev. Biol. 27, 563-584.

15. Clevers, H. (2013). The intestinal crypt, a prototype stem cell compartment. Cell 154(2), 274-284.

16. Craig, MP and Sumanas, S. (2016). ETS transcription factors in embryonic vascular development. Angiogenesis 19(3), 275-285.

17. De Biasio, A; Guarnaccia, C; Popovic, M; Uversky, AP and Pongor, S. (2008). Prevalence of intrinsic disorder in the intracellular region of human single-pass type I proteins: The case of the Notch ligand Delta-4. J. Proteome Research 7, 2496-2505.

18. Dejana, E. (2004). Endothelial cell-cell junctions: Happy together. Nature Reviews Molecular Cell Biology 5, 261-270.

19. Del Alamo, D; Rouault, H and Schweisguth, F. (2011). Mechanisms and significance of cis-inhibition in Notch signaling. Current Biology 21, R40-R47.

20. Doroquez, DB and Rebay, I. (2006). Signal integration during development: Mechanisms of EGFR and Notch pathway function and cross-talk. Crit. Rev. Biochem. and Mol. Biol. 41(6), 339-385.

21. Duryagina, R; Thieme, S; Anastassiadis, K; Werner, C; Schneider, S; Wobus, M; Brenner, S and Bornhauser, M. (2013). Overexpression of Jagged-1 and its intracellular domain in human mesenchymal stromal cells differentially affect the interaction with hematopoietic stem and progenitor cells. Stem Cells and Development 22 (20), 2736-2750.

22. Dyczynska, E; Sun, D; Yi, H; Sehara-Fujisawa, A; Blobel, CP and Zolkiewska, A. (2007).

Proteolytic processing of Delta-like 1 by ADAM proteases. The Journal of Biological Chemistry 282 (1), 436-444.

23. Erales, J and Coffino, P. (2014). Ubiquitin-independent proteosomal degradation. Biochem. Biophys. Acta 1843, 216-221.

24. Geudens, I and Gerhardt, H. (2011). Coordinating cell behavior during blood vessel formation. Development 138, 4569-4583.

25. Gomard, T; Jariel-Encontre, I; Basbous, J; Bossis, G; Moquet-Torcy, G and Piechaczyk, M. (2008). Fos family protein degradation by the proteasome. Biochemical Society Transactions 36, 858-863.

26. Guruharsha, KG; Kankel, MW and Artavanis-Tsakonas, S. (2012). The Notch signaling system: recent insights into the complexity of a conserved pathway. Nature Reviews Genetics 13, 654-666.

27. Gustafsson, MV; Zheng, X; Pereira, T; Gradin, K; Jin, S; Lundkvist, J; Ruas, JL; Poelinger, L; Lendahl, U and Bondesson, M. (2005). Hypoxia requires notch signaling to maintain the undifferentiated cell state. Dev. Cell 9(5), 617-628.

28. Herbert, SP and Stainier, DYR. (2011). Molecular control of endothelial cell behavior during blood vessel morphogenesis. Nature Reviews Molecular Cell Biology 12, 551-564.

29. Heuss, SF; Ndiaye-Lobry, D; Six, EM; Israel, A and Logeat, F. (2008). The intracellular region of Notch ligands Dll1 and Dll3 regulates their trafficking and signaling activity. PNAS 105, 11212-11217.

30. Hiratochi, M; Nagase, H; Kuramochi, Y; Koh, C-S; Ohkawara, T and Nakayama, K. (2007). The Delta intracellular domain mediates TGF-?/Activin signaling through binding to Smads and has an important bi-directional function in the Notch-Delta signaling pathway. Nucleic Acids Research 35 (3), 912-922.

31. Ikeuchi, T and Sisodia, SS. (2003). The Notch ligands, Delta1 and Jagged2, are substrates for presenelin-dependent γ-secretase cleavage. The Journal of Biological Chemistry 278 (10), 7751-7754.

32. Jin, G; Zhang, F; Chan, KM; Wong, HLX; Liu, B; Cheah, SE; Liu, X; Mauch, C, Liu, D and Zhou, Z. (2011). MT1-MMP cleaves Dll1 to negatively regulate Notch signaling to maintain normal B-cell development. EMBO J 30, 2281-2293.

33. Josten, F; Fuss, B; Felix, M; Meissner, T and Hoch, M. (2004). Cooperation of JAK/STAT and Notch signaling in the Drosophila foregut. Dev. Biol. 267(1), 181-189.

34. Jung, J; Mo, J-S; Kim, M-Y; Ann, E-J; Yoon, J-H and Park, H-S. (2011). Regulation of Notch1 signaling by Delta-like ligand 1 intracellular domain through physical interaction. Mol. Cells 32, 161-1665.

35. Kanno, T; Kamba, T; Yamasaki, T; Shibasaki, N; Saito, R; Terada, N; Toda, Y; Mikami, Y; Inoue, T; Kanematsu, A; Nishiyama, H; Ogawa, O and Nakamura, E. (2012). JunB promotes cell invasion and angiogenesis in VHL-defective renal cell carcinoma. Oncogene 31(25), 3098-110.

36. Kim, M-Y; Jung, J; Mo, J-S; Ann, E-J; Ahn, J-H; Yoon, J-H and Park, H-S. (2011). The intracellular domain of Jagged-1 interacts with Notch1 intracellular domain and promotes its degradation through Fbw7 E3 ligase. Experimental Cell Research 317, 2438-2446.

37. Kitagawa, M. (2016). Notch signaling in the nucleus: roles of Mastermind-like (MAML) transcriptional coactivators. J. Biochem. 159 (3), 287-294.

38. Kolev, V; Kacer, D; Trifonova, R; Small, D; Duarte, M; Soldi, R; Graziani, I; Sideleva, O; Larman, B; Maciag, T and Prudovsky, I. (2005). The intracellular domain of Notch ligand Delta1 induces cell growth arrest. FEBS Letters 579, 5798-5802.

39. Kopan, R and Ilagan, MXG. (2009). The canonical Notch signaling pathway: unfolding the activation. Cell 137(2), 216-233.

40. Kuhnert, F; Kirshner, JR and Thurston, G. (2011). Dll4-Notch signaling as a therapeutic target in tumor angiogenesis. Vascular Cell 3, 20.

41. LaVoie, MJ and Selkoe, DJ. (2003). The Notch ligands, Jagged and Delta, are sequentially processed by γ-secretase and presenelin/γ-secretase and release signaling fragments. Journal of

biological Chemistry 278 (36), 34427-34437.

42. Le Borgne, R; Bardin, A and Schweisguth, F. (2005). The roles of receptor and ligand endocytosis in regulating Notch signaling. Development 132(8), 1751-62.

43. Lee, H-J and Zheng, JJ. (2010). PDZ domains and their binding partners: structure, specificity and modification. Cell Comm. and Signaling 8, 8.

44. Licht, AH; Pein, OT; Florin, L; Hartenstein, B; Reuter, H; Arnold, B; Lichter, P; Angel, P and Schorpp-Kistner M. (2006). JunB is required for endothelial cell morphogenesis by regulating core-binding factor beta. J Cell Biol. 175(6), 981-91.

45. Liebler, SS; Feldner, A; Adam, MG; Korff, T, Augustin, HG and Fischer, A. (2012). No evidence for a functional role of bi-directional Notch signaling during angiogenesis. PLOS One 7 (12), e53074.

46. Luca, VC; Jude, KM; Pierce, NW; Nachury, MV; Fischer, S and Garcia, KC. (2015). Structural basis for Notch1 engagement of Delta-like 4. Science 347 (6224), 847-853.

47. Meester, JAN; Southgate, L; Stittrich, A-B; Venselaar, H; Beekmans, SJ; den Hollander, N; Bijlsma, EK; Helderman-van den Enden, A; Verheij, JB; Glusman, G; et al. (2015). Heterozygous loss-of-function nutations in DLL4 cause Adams-Oliver Syndrome. The American Journal of Human Genetics 97, 475-482.

48. Metrich, M; Pomey, AB; Berthonneche, C; Sarre, A; Nemir, M and Pedrazzini, T. (2015). Jagged1 intracellular domain-mediated inhibition of Notch1 siganalling regulates cardiac homeostasis in the postnatal heart. Cardiovascular Research 108: 74-86.

49. Nichols, JT; Miyamoto, A and Weinmaster G. (2007). Notch signaling--constantly on the move. Traffic 8(8), 959-69.

50. Palmer, WH and Deng, W-M. (2015). Ligand independent mechanisms of Notch activity. Trends in Cell Biology 25 (11), 697-707.

51. Pintar, A; DeBiasio, A; Popovic, M; Ivanova, N and Pongor, S. (2007). The intracellular region of Notch ligands: does the tail make the difference? Biology Direct 2, 19.

52. Plotnik, JP; Budka, JA; Ferris, MW and Hollenhorst, PC. (2014). ETS1 is a genome-wide effector of RAS/ERK signaling in epithelial cells. Nucleic Acid Res 42(19), 11928-11940.

53. Randi, AM; Sperone, A; Drydon, NH and Birdsey, GM. (2009). Regulation of angiogenesis by ETS transcription factors. Biochem Soc Trans 37, 1248-53.

54. Ranganathan, P; Weaver, KL and Capobianco, AJ. (2011). Notch signaling in solid tumours: a little bit of everything but not all the time. Nature Rev. Cancer 11, 338-351.

55. Roukens MG, Alloul-Ramdhani M, Baan B, kobayashi K, Peterson-Maduro J, van Dam H, Sculte-Merker S, Baker DA. (2010). Control of Endothelial Sprouting by a Tel:CtBP Complex. Nature Cell Biology 12(10), 933-942.

56. Roukens, M..G; Alloul-Ramdhani, M; Moghadasi, S; Op den Brouw, M and Baker, D.A. (2008). Downregulation of vertebrate Tel (ETV6) and Drosophila Yan is facilitated by an evolutionarily conserved mechanism of F-box-mediated ubiquitination. Mol. Cell Biol. 28, 4394–4406.

57. Roukens, M. G; Alloul-Ramdhani, M; Vertegaal, A.C; Anvarian, Z; Balog, C.I; Deelder, A.M; Hensbergen, P.J and Baker, D.A. (2008). Identification of a new site of sumoylation on Tel (ETV6) uncovers a PIAS-dependent mode of regulating Tel function. Mol. Cell Biol. 28, 2342–2357.

58. Sainson, RCA and Harris, AL. (2007). Anti-Dll4 therapy: can we block tumour growth by increasing angiogenesis. Trends in Molecular Medicine 13(9), 389-395.

59. Schorpp-Kistner, M; Wang, ZQ; Angel, P and Wagner, EF. (1999). JunB is essential for mammalian placentation. EMBO J. 18(4), 934-48.

60. Shah, AV; Birdsey, GM; Peghaire, C; Pitulescu, ME; Dufton, NP; Yang, Y; Weinberg, I; Osuna Almagro, L; Payne, L; Mason, JC; Gerhardt, H; Adams, RH and Randi, AM. (2017). The endothelial transcription factor ERG mediates Angiopoietin-1-dependent control of Notch signaling and vascular stability. Nat. Commun 8, 16002.

61. Sharghi-Namini, S; Tan, E; Sharon Ong, L-L; Ge, R and Asada, HH. (2014). DLL4-containing exosomes induce capillary sprout retraction in a 3D microenvironment. Science Reports 4, 4031.

62. Shaulian, E and Karin, M. (2001). AP-1 in cell proliferation and survival. Oncogene 20, 2390–

2400.

63. Shaulian, E and Karin, M. (2002). AP-1 as a regulator of cell life and death. Nature Cell Biology 4, 131-136.

64. Sheldon, H; Helkamp, E; Turley, H; Dragovic, R; Thomas, P; Oon, CE; Leek, R; Edelmann, M; Kessler, B; Sainson, RCA; Sargent, I; Li, J-L and Harris, AL. (2010). New mechanism of Notch signaling to endothelium at a distance by Delta-like 4 incorporation into exosomes. Blood 116 (13), 2385-2394.

65. Six, E; Ndiaye-Lobry, D; Laabi, Y; Brou, C; Gupta-Rossi, N; Israel, A and Logeat, F. (2003). The Notch ligand Delta1 is sequentially cleaved by an ADAM protease and γ-secretase. PNAS 100 (13), 7638-7643.

66. Six, EM; Ndiaye, D; Sauer, G; Laâbi, Y; Athman, R; Cumano, A; Brou, C; Israël, A and Logeat F. (2004). The notch ligand Delta1 recruits Dlg1 at cell-cell contacts and regulates cell migration. J Biol Chem. 279(53), 55818-26.

67. Sun, X and Artavanis-Tsakonas, S. (1996). The intracellular deletions of DELTA and SERRATE define dominant negative forms of the Drosophila Notch ligands. Development 122, 2465-2474.

68. Timmer, JC and Salvesen, GS. (2007). Caspase substrates. Cell Death and Differentiation 14, 66-72.

69. Ulla-Maj, F and Martinez Arias, A. (2007). Cell and molecular biology of Notch. Journal of Endocrinology 194, 459-474.

70.van Ijzendoorn, DGP; Forghany, Z; Liebelt, F; Vertegaal, AC; Jochemsen, AG; Bovée, JVMG; Szuhai, K and Baker, DA. Functional Analyses of Vascular

SUPPLEMENTARY FIGURES

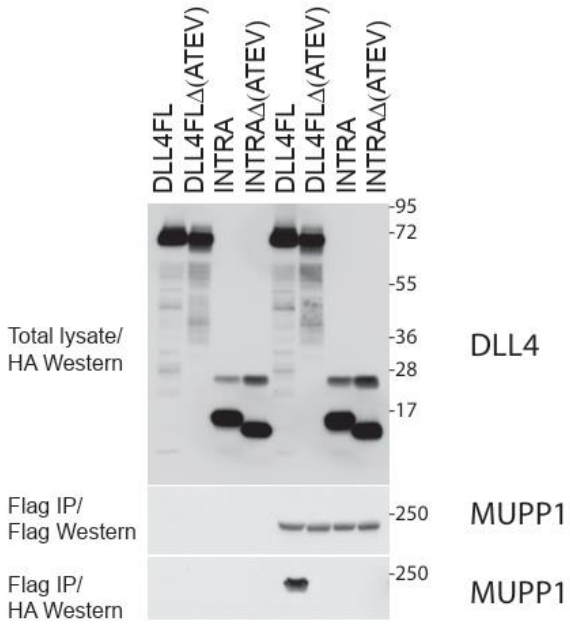

Supplementary Figure 1. MUPP1 interacts with the C-terminal PDZ-binding domain of DLL4. The indicated constructs were transfected into 293T cells. Flag epitope tagged MUPP1 was immunopurified from cell lysates using a Flag monoclonal antibody. Associated DLL4 proteins were visualized by Western blotting using an HA rabbit polyclonal antibody.

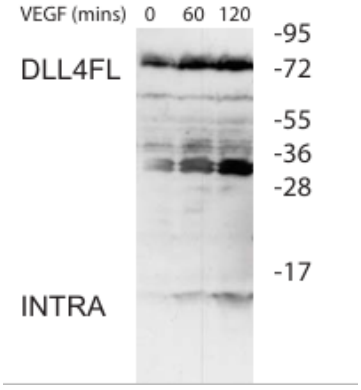

Supplementary Fig 2. HUVECs were treated with 50 ng/ml VEGF for the shown time periods. Endogenous DLL4 was immunopurified from the cells and visualized by Western blotting.

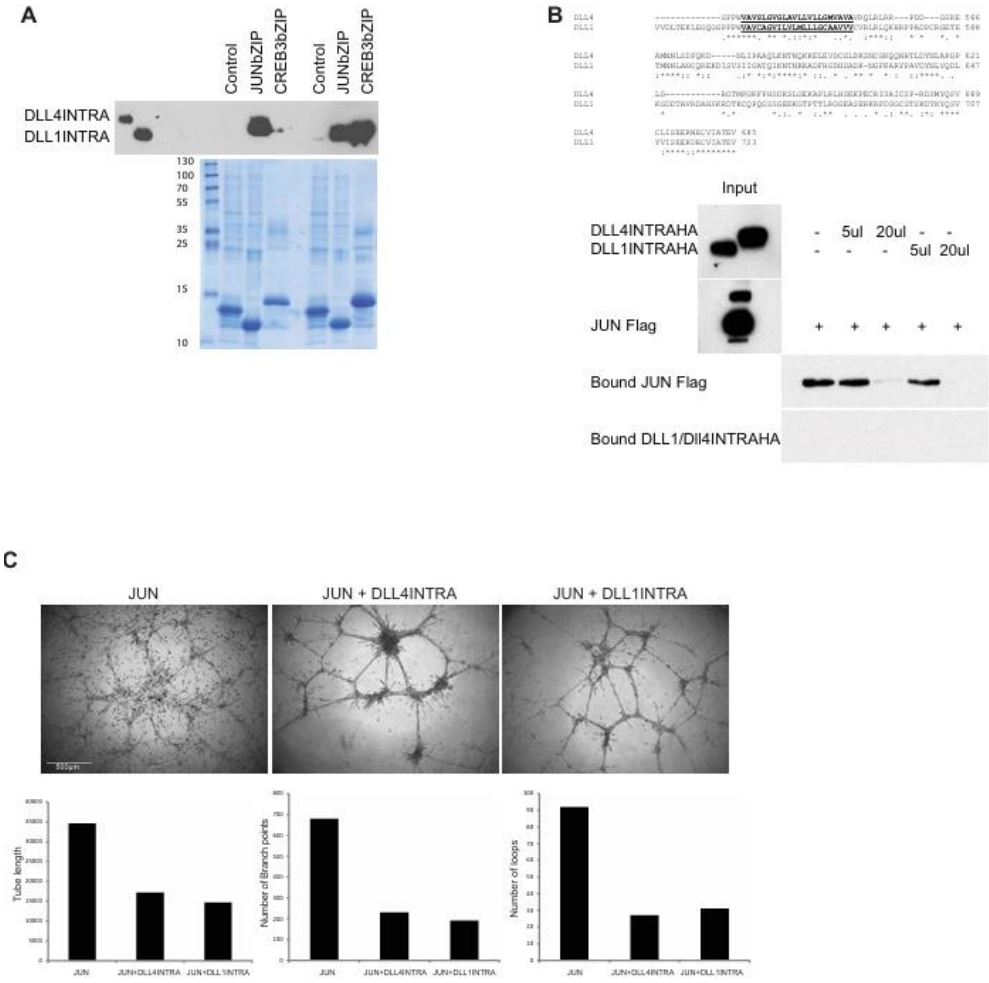

Supplementary Fig 3. (A) The ICD of DLL1 interacts biochemically with the bZIP domain of JUN. Recombinant bZIP domains of JUN and CREB3 (and a control protein) were incubated with *in vitro* translated HA epitope-tagged DLL4INTRA or DLL1INTRA. Recombinant proteins were visualized by Coomassie staining. Bound DLL4INTRA and DLL1INTRA were detected by Western blotting. **(B)** DLL1INTRA blocks JUN binding to DNA. Biotinylated AP-1 DNA binding sites were incubated with the indicated *in vitro* translated proteins. Associated JUN, DLL1 and DLL4 proteins were detected by Western blotting. **(C)** DLL1INTRA attenuates JUN-driven endothelial cell sprouting. HUVECs ectopically expressing the indicated proteins were cultured in Matrigel in the presence of 50 ng/ml VEGF. A representative of several independent experiments is shown. After 24 hours, in-house computer software was used to quantify the total length of the sprouts, the number of branch points and the number of loops. Scale bar represents 20 µM.